Supplementary Information (SI) for Catalysis Science & Technology.

Supporting Information

The synergistic effects of promoters on adjusting reaction pathway over iron catalysts for CO_2 hydrogenation to CO

Zhongtao Sun[a], Jielang Huang[a], Ling Zhou[b*], Yi Zhang[a*]

[a] College of Chemical Engineering, Beijing University of Chemical Technology, Beijing, 100029, PR China

[b] Modern Agricultural Engineering Key Laboratory at Universities of Education Department of Xinjiang Uygur Autonomous Region, Tarim University, Alar, Xinjiang Uygur Autonomous Region 843300, China

[*]Corresponding Authors: Tel &Fax:86-10-64436991

Email: zhoul-007@163.com (L.Z.); yizhang@mail.buct.edu.cn (Y.Z.)

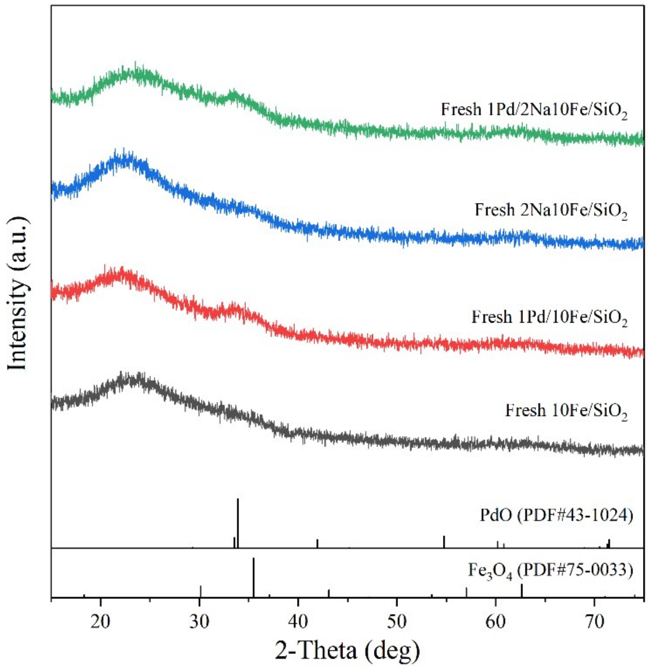

Fig. S1 XRD pattern of fresh catalysts

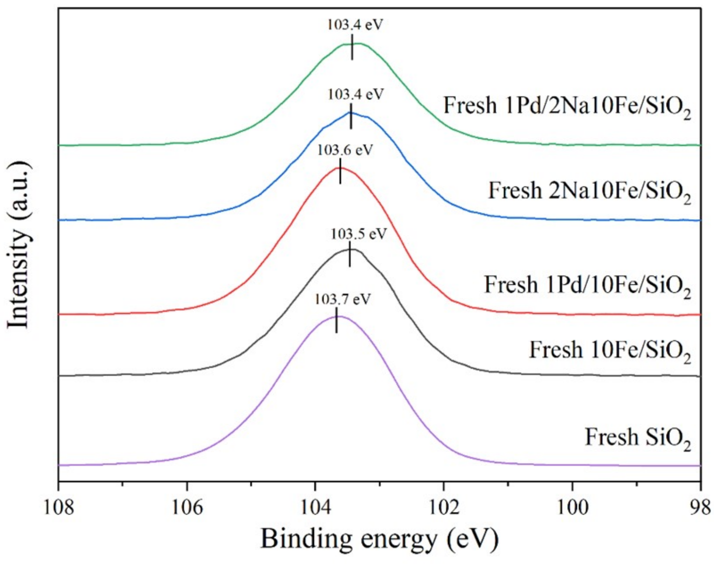

Fig. S2 Si 2p XPS spectra for various fresh catalysts

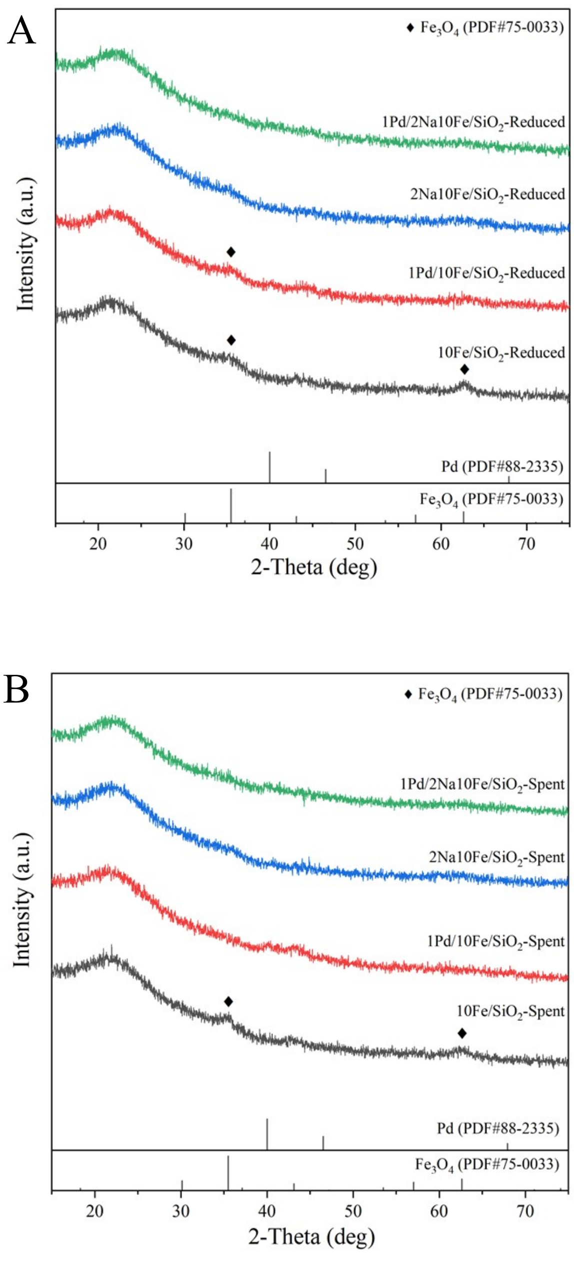

Fig. S3 XRD pattern of reduced and spent catalysts. (A) reduced catalysts, (B) spent catalysts

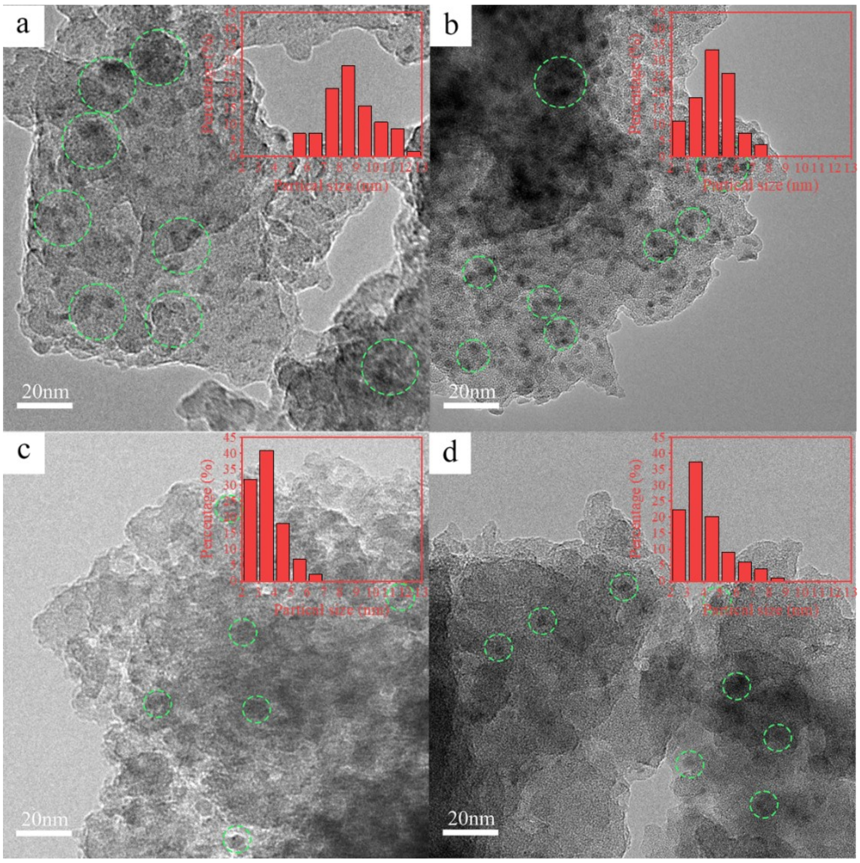

Fig. S4 TEM images of different spent catalysts: (a) $10Fe/SiO_2$; (b) $1Pd/10Fe/SiO_2$; (c) $2Na10Fe/SiO_2$; (d) $1Pd/2Na10Fe/SiO_2$

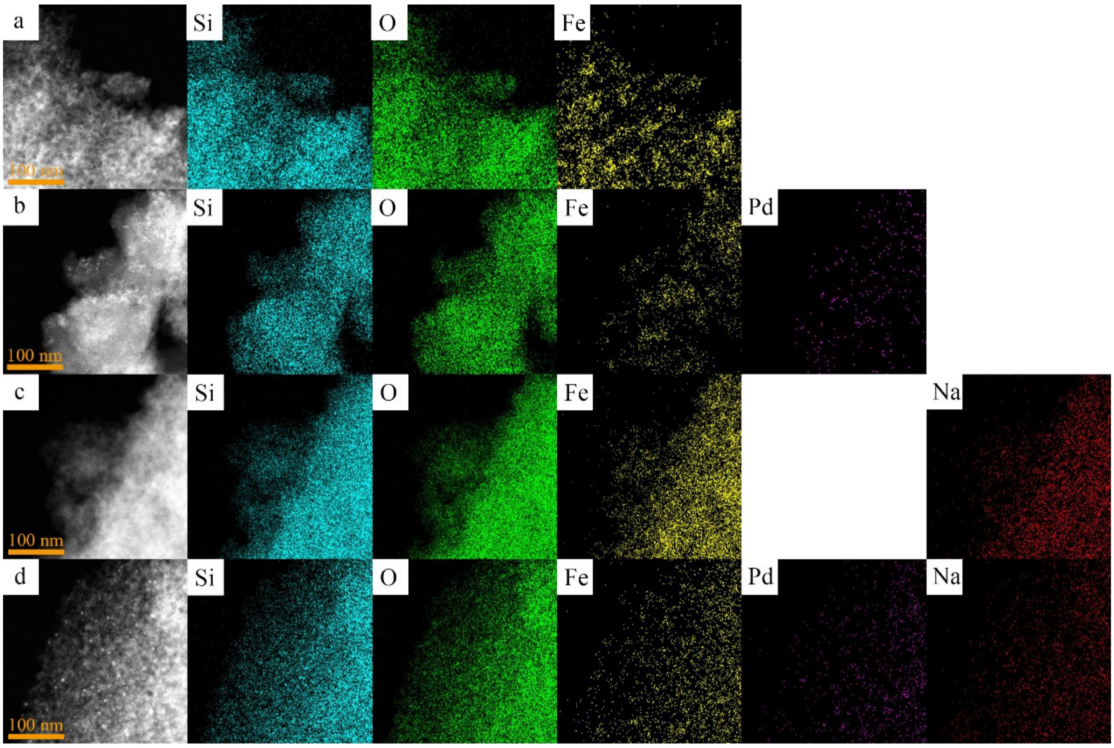

Fig. S5 STEM-EDX elemental mapping of different spent catalysts: (a) 10Fe/SiO_2; (b) 1Pd/10Fe/SiO_2; (c) 2Na10Fe/SiO_2; (d) 1Pd/2Na10Fe/SiO_2

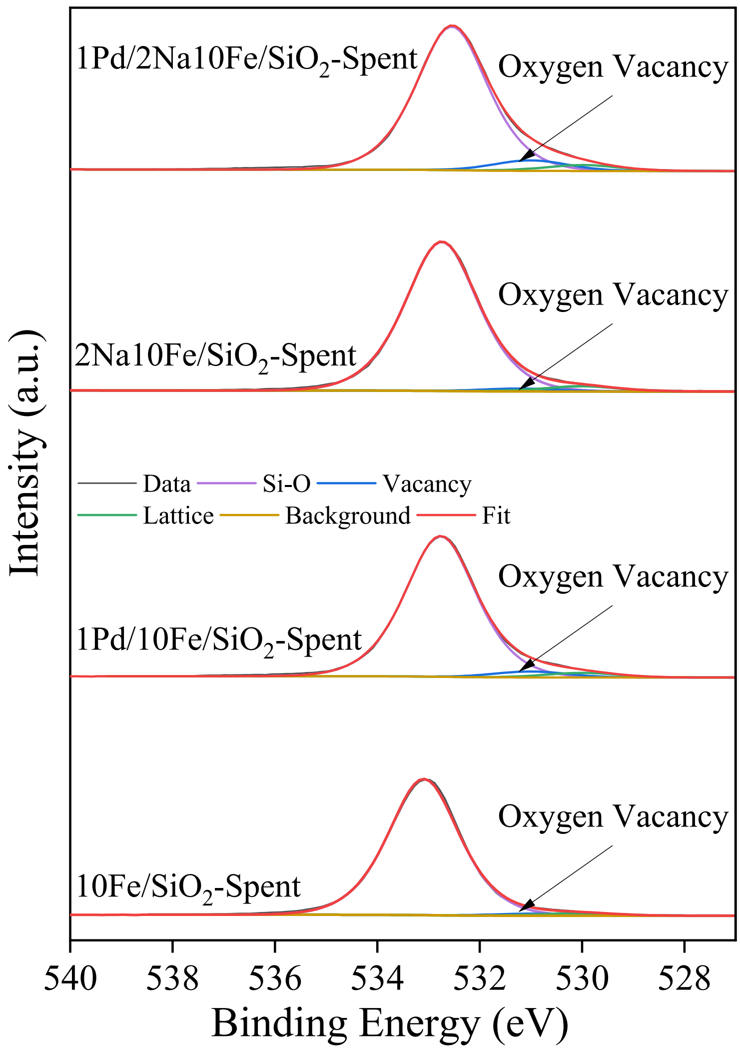

Fig. S6 O 1s XPS spectra for various spent catalysts

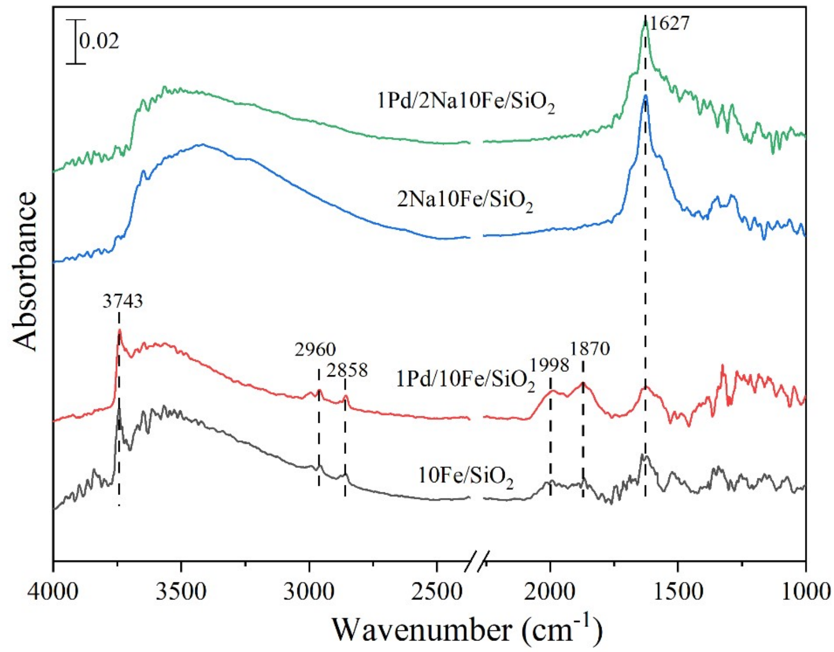

Fig. S7 In situ CO_2-DRIFTS results after CO_2 adsorption for various catalysts

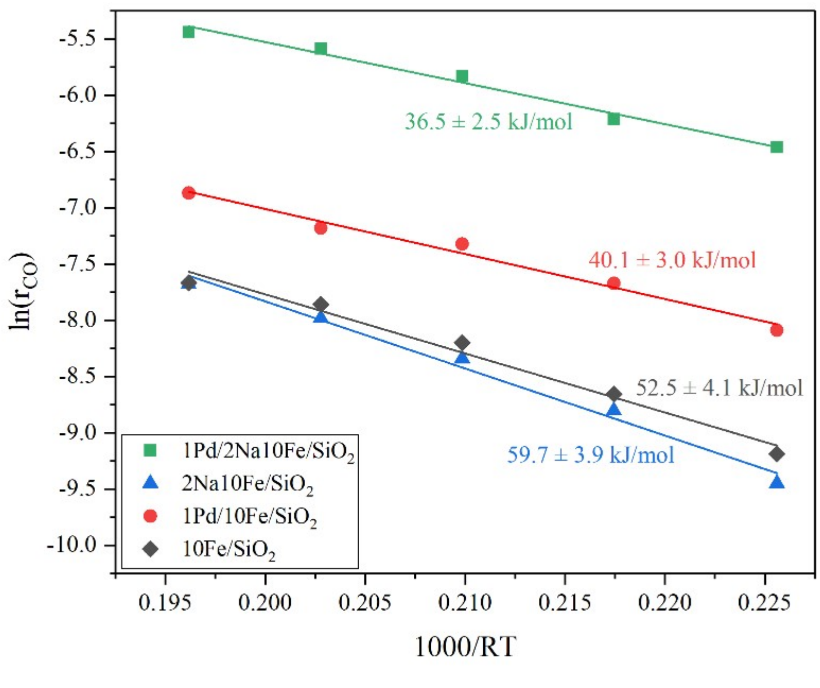

Fig. S8 Arrhenius plot for various catalysts

Table S1. Catalytic performance of as-prepared catalysts [a].

Catalysts	Conv. (%) CO_2	Sel. (%) CO	Sel. (%) C_xH_y [b]	Sel. (%) C_xH_yOH [c]
10Fe/SiO_2	2.8	46.4	46.5	7.1
1Pd/10Fe/SiO_2	6.3	42.8	48.8	8.4
2Na10Fe/SiO_2	1.0	93.5	4.7	1.8
1Pd/2Na10Fe/SiO_2	13.2	99.7	0.1	0.2
1Pd/SiO_2	5.5	92.7	0.6	6.7

[a] Reaction conditions: 300℃, 3.0 MPa, H_2/CO_2 = 3, GHSV = 1600 mL/g_{cat} h^{-1}.

[b] Include C_1-C_7 hydrocarbon.

[c] Include C_1-C_3 alcohol.

Table S2. Elemental compositions of as-prepared detected by XRF and ICP-OES.

Samples	Weight content [a] (%)					Weight content of different species [b] (%)		
	O	Si	Fe	Na	Pd	Fe	Na	Pd
10Fe/SiO_2	49.6	39.3	11.0	0.0	0.0	9.00	-	-
1Pd/10Fe/SiO_2	49.2	38.9	11.1	0.0	0.9	8.12	-	0.71
2Na10Fe/SiO_2	49.1	38.4	10.9	1.6	0.0	8.67	1.75	-
1Pd/2Na10Fe/SiO_2	48.5	37.7	11.2	1.7	0.9	8.41	1.73	0.70

[a] detected by XRF.

[b] detected by ICP-OES.

Table S3. Physical properties of as-prepared catalysts.

Samples	Surface area[a] (m^2/g)	Pore volume[b] (cm^3/g)	Pore size[b] (nm)
SiO_2	496.4	0.78	4.9
$10Fe/SiO_2$	414.6	0.58	5.6
$1Pd/10Fe/SiO_2$	409.6	0.59	4.9
$2Na10Fe/SiO_2$	339.4	0.58	5.6
$1Pd/2Na10Fe/SiO_2$	348.9	0.55	4.9

a calculated by BET method

b calculated by BJH method

Table S4. The results of XPS for Fe $2p_{3/2}$

Catalysts	Binding energy (eV) Fe $2p_{3/2}$		Content (atom%)	
	Fe^{2+}	Fe^{3+}	Fe^{2+}	Fe^{3+}
$10Fe/SiO_2$-Reduced	710.2	711.5	6.6	93.4
$1Pd/10Fe/SiO_2$-Reduced	709.8	711.3	14.8	85.2
$2Na10Fe/SiO_2$-Reduced	709.6	711.3	4.2	95.8
$1Pd/2Na10Fe/SiO_2$-Reduced	709.5	711.3	10.2	89.8
$10Fe/SiO_2$-Spent	710.1	711.5	17.2	82.8
$1Pd/10Fe/SiO_2$-Spent	709.7	711.4	27.1	72.9
$2Na10Fe/SiO_2$-Spent	709.6	711.5	16.0	84.0
$1Pd/2Na10Fe/SiO_2$-Spent	709.5	711.3	23.1	76.9

Table S5. The results of XPS for O 1s

Catalysts	Binding energy (eV) O 1s			Content (atom%)		
	Si-O	Vacancy	Lattice	Si-O	Vacancy	Lattice
10Fe/SiO_2-Spent	533.1	531.0	530.0	97.1	0.1	0.2
1Pd/10Fe/SiO_2-Spent	532.8	531.0	530.0	93.4	3.7	2.9
2Na10Fe/SiO_2-Spent	532.7	531.0	530.0	95.3	0.8	3.9
1Pd/2Na10Fe/SiO_2-Spent	532.6	531.0	530.0	90.1	6.3	3.6

The peak at about 530.0, 531.0, 532.8 eV corresponded to the lattice oxygen of iron oxides, the oxygen defects and lattice oxygen of Si-O species[1–3]. The density of oxygen vacancies could be reflected by content of oxygen defects[4,5]. As shown in Fig. S6 and Table S5, the density of oxygen defects ranked in the following order: 1Pd/2Na10Fe/SiO_2 > 1Pd/10Fe/SiO_2 > 2Na10Fe/SiO_2 > 10Fe/SiO_2, indicating the Pd species could facilitate the formation of oxygen vacancies.

Table S6. Mössbauer parameters of the reduced and spent catalysts

Catalysts	Phases	Mössbauer parameters		
		IS (mm/s)	QS (mm/s)	Area (%)
$10Fe/SiO_2$-Reduced	Fe^{2+}(spm)	0.70	1.10	7.0
	Fe^{3+}(spm)	0.34	0.82	93.0
$1Pd/10Fe/SiO_2$-Reduced	Fe^{2+}(spm)	0.93	1.60	15.6
	Fe^{3+}(spm)	0.33	0.99	84.4
$2Na10Fe/SiO_2$-Reduced	Fe^{2+}(spm)	1.17	1.85	4.1
	Fe^{3+}(spm)	0.34	0.88	95.9
$1Pd/2Na10Fe/SiO_2$-Reduced	Fe^{2+}(spm)	0.71	2.00	12.4
	Fe^{3+}(spm)	0.36	0.84	87.6
$10Fe/SiO_2$-Spent	Fe^{2+}(spm)	0.70	0.98	19.2
	Fe^{3+}(spm)	0.33	0.86	80.8
$1Pd/10Fe/SiO_2$-Spent	Fe^{2+}(spm)	1.11	1.94	32.2
	Fe^{3+}(spm)	0.33	0.98	67.8
$2Na10Fe/SiO_2$-Spent	Fe^{2+}(spm)	0.93	1.60	17.3
	Fe^{3+}(spm)	0.33	0.99	82.7
$1Pd/2Na10Fe/SiO_2$-Spent	Fe^{2+}(spm)	1.08	1.89	29.0
	Fe^{3+}(spm)	0.35	0.90	71.0

Table S7. The results of XPS for Pd $3d_{5/2}$

Catal.	Binding energy (eV) Pd $3d_{5/2}$			Content (atom%)		
	Pd^0	$Pd^{\delta+}$	Pd^{2+}	Pd^0	$Pd^{\delta+}$	Pd^{2+}
$1Pd/10Fe/SiO_2$-Reduced	335.1	-	337.0	80.0	-	20.0
$1Pd/2Na10Fe/SiO_2$-Reduced	335.0	-	336.7	82.0	-	18.0
$1Pd/10Fe/SiO_2$-Spent	335.1	-	336.8	75.0	-	25.0
$1Pd/2Na10Fe/SiO_2$-Spent	334.6	335.5	336.7	51.0	25.0	24.0

Table S8. The integration results of CO_2-TPD profiles

Catalysts	Peak area (a.u.)			Content (%)		
	Weak basic sites	Medium basic sites	Strong basic sites	Weak basic sites	Medium basic sites	Strong basic sites
10Fe/SiO_2-Spent	1129	1861	2285	21.4	35.3	43.3
1Pd/10Fe/SiO_2-Spent	908	3169	2666	13.5	47.0	39.5
2Na10Fe/SiO_2-Spent	1708	3713	2143	22.6	49.1	28.3
1Pd/2Na10Fe/SiO_2-Spent	1419	4025	3478	15.9	45.1	39.0

(1) Lu, F.; Chen, X.; Wang, W.; Zhang, Y. Adjusting the CO_2 Hydrogenation Pathway via the Synergic Effects of Iron Carbides and Iron Oxides. *Catal. Sci. Technol.* **2021**, *11* (23), 7694–7703. https://doi.org/10.1039/D1CY01758F.

(2) Chen, Y.; Wang, C.; Liu, Y.; Zhang, Q.; Zhou, L.; Zhang, Y. The Pd/ZrO_2 Catalyst Inversely Loaded with Various Metal Oxides for Methanol Synthesis from Carbon Dioxide. *J. Catal.* **2024**, *434*, 115527. https://doi.org/10.1016/j.jcat.2024.115527.

(3) Paparazzo, E. XPS Analysis of Oxides. *Surf. Interface Anal.* **1988**, *12* (2), 115–118. https://doi.org/10.1002/sia.740120210.

(4) Huang, C.; Wu, Z.; Luo, H.; Zhang, S.; Shao, Z.; Wang, H.; Sun, Y. CO_2 Hydrogenation to Methanol over PdZnZr Solid Solution: Effects of the PdZn Alloy and Oxygen Vacancy. *ACS Appl. Energy Mater.* **2021**, *4* (9), 9258–9266. https://doi.org/10.1021/acsaem.1c01502.

(5) Jiang, F.; Wang, S.; Liu, B.; Liu, J.; Wang, L.; Xiao, Y.; Xu, Y.; Liu, X. Insights into the Influence of CeO_2 Crystal Facet on CO_2 Hydrogenation to Methanol over Pd/CeO_2 Catalysts. *ACS Catal.* **2020**, *10* (19), 11493–11509. https://doi.org/10.1021/acscatal.0c03324.